

Research on dynamic characteristics of wind turbine hybrid towers under environmental influences based on operational modal identification and refined finite element simulation

Original

Research on dynamic characteristics of wind turbine hybrid towers under environmental influences based on operational modal identification and refined finite element simulation / Xing, Kankan; Zhang, Zhenli; Tang, Shengbo; Jiang, Weitao; Lacidogna, Giuseppe; Xu, Jie. - In: FRONTIERS IN BUILT ENVIRONMENT. - ISSN 2297-3362. - STAMPA. - 11:(2026), pp. 1-21. [10.3389/fbuil.2025.1728006]

Availability:

This version is available at: 11583/3006916 since: 2026-01-25T09:32:12Z

Publisher:

Frontiers Media

Published

DOI:10.3389/fbuil.2025.1728006

Terms of use:

This article is made available under terms and conditions as specified in the corresponding bibliographic description in the repository

Publisher copyright

(Article begins on next page)



OPEN ACCESS

EDITED BY

Jian Li,
University of Kansas, United States

REVIEWED BY

You Dong,
Hong Kong Polytechnic University, Hong
Kong SAR, China
Kareem Eltoumy,
Simpson Gumpertz and Heger Inc.,
United States
Zhen Sun,
Southeast University, China

*CORRESPONDENCE

Jie Xu,
✉ jxu@tju.edu.cn

RECEIVED 19 October 2025

REVISED 22 November 2025

ACCEPTED 02 December 2025

PUBLISHED 02 January 2026

CITATION

Xing K, Zhang Z, Tang S, Jiang W, Lacidogna G
and Xu J (2026) Research on dynamic
characteristics of wind turbine hybrid towers
under environmental influences based on
operational modal identification and refined
finite element simulation.
Front. Built Environ. 11:1728006.
doi: 10.3389/fbuil.2025.1728006

COPYRIGHT

© 2026 Xing, Zhang, Tang, Jiang, Lacidogna
and Xu. This is an open-access article
distributed under the terms of the [Creative
Commons Attribution License \(CC BY\)](https://creativecommons.org/licenses/by/4.0/). The
use, distribution or reproduction in other
forums is permitted, provided the original
author(s) and the copyright owner(s) are
credited and that the original publication in
this journal is cited, in accordance with
accepted academic practice. No use,
distribution or reproduction is permitted
which does not comply with these terms.

Research on dynamic characteristics of wind turbine hybrid towers under environmental influences based on operational modal identification and refined finite element simulation

Kankan Xing¹, Zhenli Zhang¹, Shengbo Tang², Weitao Jiang^{2,3},
Giuseppe Lacidogna⁴ and Jie Xu^{2*}

¹Shandong Electric Power Engineering Consulting Institute Corp., Ltd., Jinan, China, ²School of Civil Engineering, Tianjin University, Tianjin, China, ³Tianjin Qiushi Intelligent Technology Corp., Ltd., Tianjin, China, ⁴Department of Structural, Geotechnical and Building Engineering, Politecnico di Torino, Torino, Italy

As hybrid towers of wind turbines have gradually become the mainstream structural configuration for high-power wind turbines, their structural safety and long-term reliability have increasingly become critical issues. However, existing studies have insufficiently focused on the impacts of environmental factors and local structural characteristics on hybrid tower structures. To address this gap, this study conducts research on the dynamic characteristics of wind turbine hybrid towers based on Operational Modal Analysis (OMA) and finite element simulation. This study proposes a systematic operational modal analysis process: compared with traditional modal identification methods, this study combines the Frequency Domain Decomposition (FDD) method and the Stochastic Subspace Identification-Covariance (SSI-COV) method to achieve effective extraction of structural modal frequencies and mode shapes under operational conditions. Through the progressive strategy of preliminary identification-accurate estimation-spurious mode elimination, this process significantly improves the efficiency and accuracy of modal parameter identification. The analysis results show that within the range of conventional environmental variations, no significant statistical correlation is observed between the identified modal parameters (frequency, mode shape) and environmental factors (wind direction, wind speed, temperature). It should be noted that the validity of these conclusions is limited to the specific environmental conditions and data acquisition periods investigated in this study—namely, wind speeds of 2.0–5.5 m/s, temperatures of 17 °C–35.8 °C, wind direction variations of approximately 10°, and data collected daily between 11:45 and 12:15—without encompassing seasonal-scale extreme environmental variations. Meanwhile, this study establishes a finite element model of the wind turbine hybrid tower and verifies its effectiveness using on-site measured data. Parametric analysis and damage simulation based on the validated model reveal that the elastic modulus of concrete is the

most sensitive parameter affecting the overall dynamic characteristics of the structure, compared with the elastic moduli of steel and foundation. Additionally, the influence of stiffness degradation in different regions of the concrete tower on the natural frequencies of each order is related to the specific location of damage and the modal order of structural vibration. The conclusions of this study provide a theoretical basis for the optimal design of wind turbine hybrid tower structures and offer important references for formulating structural health monitoring strategies based on dynamic characteristics.

KEYWORDS

wind turbine hybrid tower, operational modal identification, finite element simulation, environmental influence, dynamic characteristics

1 Introduction

In the global joint efforts to address climate change and promote the transformation of the energy structure towards cleanliness and low carbon, wind power generation, as one of the most mature and cost-effective renewable energy sources, is experiencing unprecedented rapid development (Van de Graaf, 2014, p. 492; Global Wind Energy Council, 2021, p. 80). To maximize energy capture efficiency and continuously reduce the Levelized Cost of Energy (LCoE) throughout the entire project life cycle, modern onshore wind turbine technology shows a clear trend of large-scale development, that is, using longer blades and higher hubs (Wiser et al., 2023; Bórawski et al., 2020). Especially in inland areas with relatively weak wind resources, increasing the hub height to reach wind layers at higher altitudes with more stable wind speeds and smaller turbulence effects has become a key strategy to increase power generation and expand the geographical boundaries of wind power development (Lantz et al., 2019; Burton et al., 2011).

This technological trend has spawned an urgent need for ultra-high towers of 140 m or even 160 m and above. When the hub height exceeds 120 meters, the traditional all-steel tubular tower faces severe transportation bottlenecks due to its excessively large bottom diameter. The steel-concrete hybrid tower (hybrid tower), composed of a lower concrete section and an upper steel section, has emerged as the times require and quickly become the mainstream technical solution for high-pile towers (Tapoglou et al., 2025; Cheng, Zhao, Qi and Zhou, 2024). However, the hybrid tower is not a simple material replacement, but a shift in structural paradigm. The heterogeneity of its materials, the key steel-concrete connection section as a complex area of mechanical behavior, and the complex prestress system applied to the concrete cylinder jointly introduce dynamic behaviors completely different from those of traditional homogeneous steel towers (Zhang et al., 2024; Ribeiro et al., 2025). Therefore, the design experience and analysis models established for medium and low-height steel towers in the past are no longer fully applicable. It is crucial to conduct in-depth research on the dynamic characteristics of such new structures and establish a Structural Health Monitoring (SHM) strategy throughout their design, construction, and operation and maintenance cycles (Ciang, Lee and Bang, 2008; Yang, Liang, Zhu and Zhang, 2024).

SHM technology based on vibration monitoring is the core means to ensure the safety of large civil engineering structures. Among them, Operational Modal Analysis (OMA) can identify

the dynamic characteristics of a structure only by using the environmental excitation (such as wind, microseism, etc.) of the structure in service. Due to its advantages of being economical, convenient, and not interrupting the normal operation of the structure, it has become the standard method for evaluating the dynamic characteristics of in-service structures (Brincker and Ventura, 2015; Rainieri and Fabbrocino, 2014). Among many OMA technologies, the Frequency Domain Decomposition (FDD) method and the Stochastic Subspace Identification (SSI) method are the two most widely used and mature technologies at present. FDD has high calculation efficiency and can quickly provide accurate estimates of the natural frequency of the structure, while SSI, as a time-domain parameterization method, can more accurately identify a full set of modal parameters including the damping ratio. The combination of the two has become the best practice in OMA analysis (Zhang et al., 2023; Reynders, 2012). The core idea of this method is that the modal parameters of a structure are a direct reflection of its physical properties (mass, stiffness, damping). Therefore, by tracking the small changes of these parameters, the change of the structural health state can be inferred reversely, so as to realize early warning of potential damage (Sharma et al., 2021).

However, this technology faces a core challenge in practical applications: the complex variability of Environmental and Operational Conditions (EOCs). Changes in environmental factors such as temperature, wind speed, and humidity can also cause fluctuations in modal parameters, and their influence sometimes even drowns out the weak signals caused by early damage, resulting in serious misjudgment or missed judgment (Sohn, 2007). In the field of bridge engineering, a large number of studies have confirmed that temperature is the most important factor affecting modal frequency. It affects the structural stiffness by changing the elastic modulus of materials (especially concrete). This alone can cause a significant annual periodic change of up to 5%–15% in the natural frequency of the structure (Mosavi et al., 2012). For offshore wind turbines, their dynamic characteristics are affected by the complex coupling of wind speed, waves, currents, and impeller speed. For example, the increase in operating wind speed will introduce significant aerodynamic damping, thereby changing the damping ratio and natural frequency of the structure (Dong et al., 2014; Partovi-Mehr et al., 2022). To meet this challenge, the academic community has invested a lot of energy in developing complex environmental effect stripping algorithms. These methods, from traditional multiple linear regression and Principal Component



FIGURE 1 Overall architecture of wind turbine hybrid tower monitoring system.

TABLE 1 Material parameters of wind turbine hybrid tower.

Material	Density/kg/m ³	Elastic modulus/MPa	Poisson's ratio	Yield stress/MPa
HRB500	7,850	2.00×10^5	0.3	435
Q355	7,850	2.06×10^5	0.3	355
Steel strand	7,850	1.95×10^5	0.3	1,320
C50	2,500	3.55×10^4	0.2	-
C80	2,500	4.09×10^4	0.2	-
C95	2,500	4.33×10^4	0.2	-
C105	2,500	4.48×10^4	0.2	-

TABLE 2 Geometric parameters of wind turbine hybrid tower.

Tower section number	Outer diameter of bottom surface/mm	Outer diameter of top surface/mm	Thickness/mm	Height/mm
M1-M7	7,800	7,800	300	4,000
M8	7,800	6,600	300	4,000
M9-M14	6,600	6,600	300	4,000
M15	6,600	5,400	300	4,000
M16-M26	5,400	5,400	300	4,000
M27	5,400	4,900	300	4,000
M28	4,900	4,600	650	2,400
Steel transition section	4,500	4,470	30	3,026
S1	4,470	4,470	20	18,600
S2	4,470	3,900	20	25,000

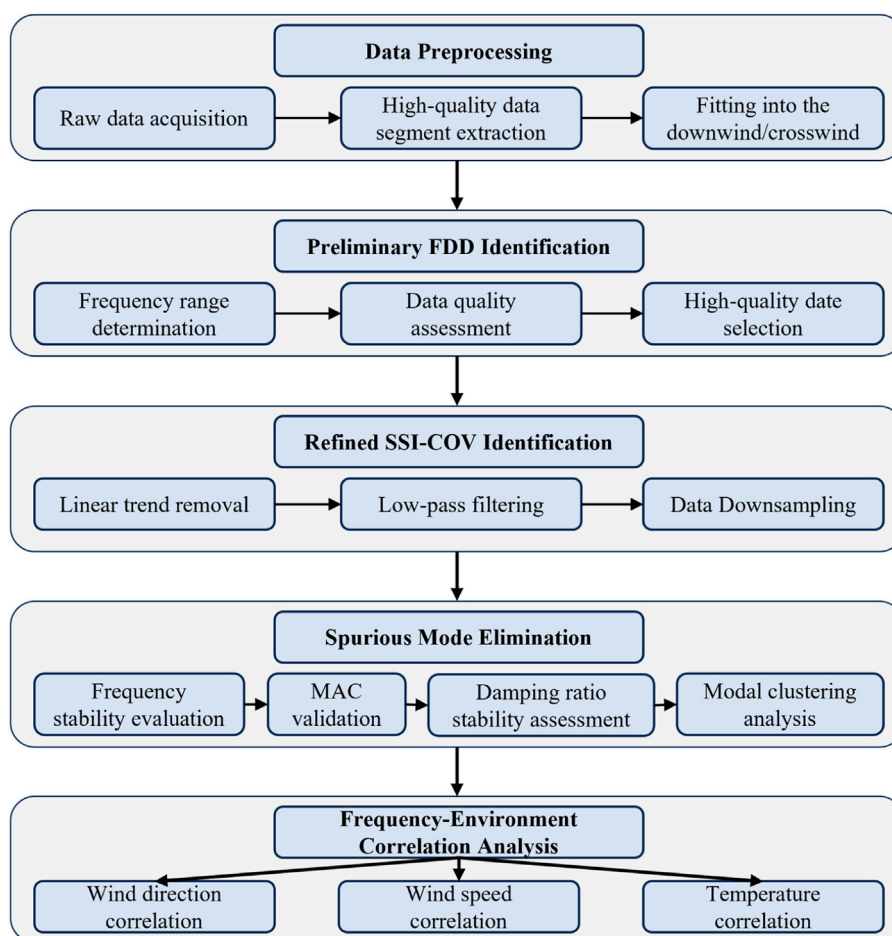


FIGURE 2
Modal analysis process of wind turbine hybrid tower.

Analysis (PCA) to advanced methods based on machine learning in recent years, such as Support Vector Machine (SVM), Gaussian Process Regression (GPR), and Deep Neural Network (DNN), all aim to establish a complex nonlinear relationship model between modal parameters and EOCs from monitoring data, thereby filtering out environmental “noise” and purifying damage “signals” (Pei et al., 2025; Lenzen et al., 2021). These data-driven methods, especially from the perspective of machine learning, provide a powerful framework for identifying damage-sensitive features (Farrar and Worden, 2012; Reuland et al., 2023). In addition, the high-precision Finite Element (FE) model, as a “digital twin” tool, plays a key role in damage simulation (for example, by analyzing the stiffness reduction effect) and mechanism analysis (Asmine et al., 2010; Aikhuele and Diemuodeke, 2024). Existing studies have verified the reliability of FE models in structural performance analysis by establishing a 3D FE model of the foundation-soil-anchor bolt system and simulating foundation damage evolution using the Concrete Damage Plasticity (CDP) model, providing a reference for the “digital twin” construction of hybrid towers (Zhang et al., 2023). However, its reliability relies heavily on the verification and update of field measured data, and this process also needs to accurately handle the influence of EOCs.

Although rich results have been achieved in research, the existing literature system still has obvious knowledge gaps when applied to the SHM of high-pile onshore hybrid towers. First of all, current research on the influence of EOCs mainly focuses on bridges and offshore wind turbines. As a new type of structure with huge thermal inertia and relatively single onshore stress state, whether the sensitivity of high-pile onshore hybrid towers to EOCs is consistent with other structure types still lacks verification from long-term measured data. Secondly, as a high-fidelity “digital twin” model for damage simulation and mechanism analysis, the currently publicly available hybrid tower models that have been strictly verified by field data are extremely scarce—existing studies have conducted refined FE modeling for hybrid tower foundations, analyzed structural safety under different working conditions, and optimized weak parts (Liu et al., 2023), but high-fidelity models for the entire hybrid tower structure (especially steel-concrete composite towers) are still rare, which limits the reliability of most numerical analyses. Furthermore, studies on local characteristics of hybrid towers, such as the mechanical performance of wet-connected prefabricated steel-concrete composite towers (Jia et al., 2025) and the application of prestressing technology in foundation slabs (Liu et al., 2024), have provided a basis for key part design but not yet connected with

TABLE 3 Meteorological data and date selection for wind turbine hybrid tower.

Date	Average wind speed/m/s ²	12:00 average wind direction angle/deg	Maximum temperature/°C	Minimum temperature/°C	Whether selected
20250728	4.62	178.1	35.3	28.4	No
20250729	4.19	180.55	35.9	28.3	No
20250730	3.89	179.6	33.2	28.7	No
20250731	7.37	181.2	31.1	26.2	No
20250801	5.31	178.3	30.78	26.5	No
20250802	4.06	179.5	32.6	27.1	Yes
20250803	1.77	236.94	39.4	28.7	No
20250804	4.08	186.63	38.7	31.5	Yes
20250805	5.19	179.43	36.3	31.3	Yes
20250806	2.44	183.69	41.2	32.1	Yes
20250807	2.08	229.51	37.84	29.6	No
20250808	1.54	205.17	35.8	29.8	No
20250809	5.08	186.91	32.9	27	Yes
20250810	3.61	180.6	30	26.1	Yes
20250811	4.13	184.03	26.7	24.9	No
20250812	2.84	180.08	28.1	25.4	Yes
20250813	2.03	184.7	33.6	25.9	Yes
20250814	4.45	143.6	37.1	28	Yes
20250815	4.09	178.08	29.9	29.27	Yes
20250816	3.59	180.01	40	31	No

overall structural dynamic monitoring, making it difficult to support local damage identification based on modal parameters. This *status quo* directly leads to the third deficiency: the theoretically damage-sensitive high-order modal damage identification method for local damage is difficult to determine the best modal index for monitoring key parts (such as the steel-concrete connection section) due to the lack of a reliable model for sensitivity analysis, so its practical application is seriously restricted.

To meet the above challenges and fill key research gaps, this paper conducts a comprehensive study on the dynamic characteristics of an in-service 160-m-high wind turbine hybrid tower. This study aims to make the following three core contributions through a combination of experiments and numerical simulations:

1. Confirm the limited influence of environmental factors: Through long-term on-site vibration monitoring and advanced OMA technology, it is empirically confirmed for the first time that

under normal operating conditions, environmental factors have no significant influence on the modal frequency of high-pile onshore hybrid towers. This finding provides an important prerequisite for the SHM of such structures, that is, the significant changes in modal frequency can be more reliably attributed to changes in the structure's own state, thereby simplifying the damage identification algorithm.

2. Construction of a high-fidelity finite element benchmark model: Based on detailed engineering data, a high-precision finite element model was established and validated. This model not only provides a solid foundation for the parametric analysis in the present study but also serves as a valuable reference tool for the engineering design and scientific research of similar structures.
3. Reveal the sensitivity of key parameters and evaluate damage identifiability: Using the verified model, the high sensitivity of key design parameters such as the elastic modulus of

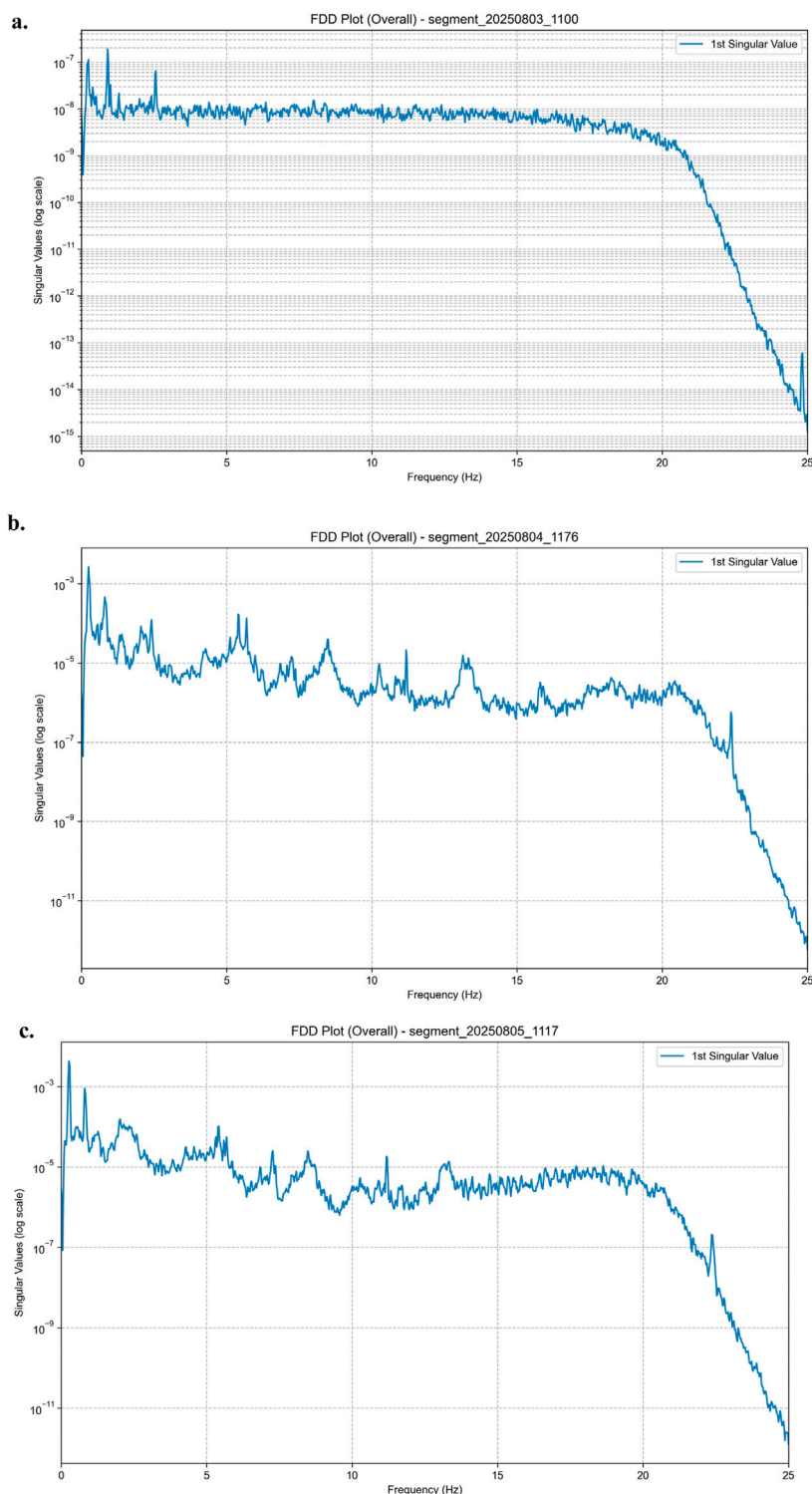


FIGURE 3 Comparison of FDD Spectra Quality and Criteria for High-Quality Data Selection. **(a)** 8.3 Frequency data. **(b)** 8.4 Frequency data. **(c)** 8.5 Frequency data.

concrete to the dynamic characteristics of the structure is systematically revealed. More importantly, through damage simulation, it is clarified that there is a unique “position-order” correspondence between the stiffness degradation at

different positions and the frequency changes of each order of modes, which lays a theoretical foundation for the future development of damage identification and evaluation methods based on multi-order frequency modes.

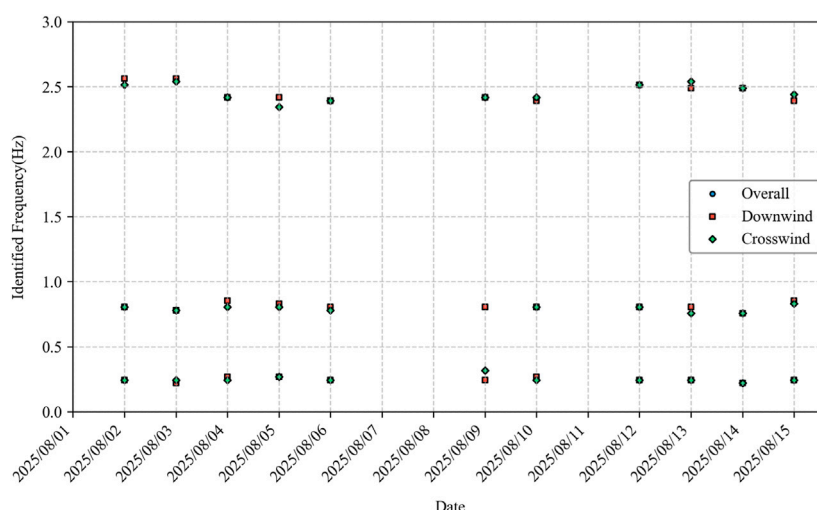


FIGURE 4 Analysis of the relationship between wind direction and frequency of wind turbine hybrid tower by FDD.

2 Operational modal analysis and assessment of environmental effects

2.1 Description of the hybrid tower and measurement system

The wind turbine structure studied in this paper is located in a certain area of Yingshang, Anhui Province, with a rated power of 5.27 MW and a hub center height of 160 m. As shown in Figure 1, the wind turbine structure is mainly composed of a Steel Tower Section, a Concrete Tower Section, and a foundation. Among them, the Concrete Tower Section is a prefabricated assembled structure, consisting of 28 ring segments in total—starting from the first ring (M1) at the top of the foundation to the 28th ring (M28) at the bottom of the Steel Tower Section. The segments are connected through a wet-joint method using inserted bars and grouting; meanwhile, external prestressed steel strands are used to enhance the integrity of each assembled section of the hybrid tower. The Steel Tower Section is divided into two subsections, namely, S1 and S2. Specifically, the hybrid tower has a height of 110.40 m (comprising 28 segments in total), the Steel Tower Section has a height of 43.76 m, the blade diameter is 189.40 m, and the foundation adopts a pile-cap type. The material parameters of the models for different tower sections are shown in Table 1, while the detailed geometric parameters are provided in Table 2.

To accurately capture the dynamic response of the wind turbine hybrid tower under operating conditions, this study adopted a structural health monitoring system based on force-balanced acceleration sensing technology. The core equipment of this system is a three-component force-balanced acceleration sensor (Model: WG-FBA03), which is equipped with three orthogonal measurement channels: east-west (X), south-north (Y), and vertical (Z), and can simultaneously record acceleration responses in the three directions. A supporting 16-channel Data Acquisition

Instrument is used for data collection, and the overall architecture of the system is shown in Figure 1. The monitoring system uses three-component force-balanced acceleration sensors, and the sampling frequency is set to 200 Hz.

The sensor deployment scheme is designed based on the structural dynamic characteristics and the local wind environment. According to meteorological data, the prevailing wind direction in Yingshang County, Fuyang City, Anhui Province is easterly; therefore, the X-axis of all sensors is uniformly oriented eastward and the Y-axis northward to ensure accurate capture of along-wind and cross-wind vibration responses. As a cantilever-type flexible structure, the tower exhibits vibration responses characterized by larger amplitudes at the top and smaller amplitudes at the base, yet the base vibration directly reflects the essential constraint nature of the tower–foundation coupled system. Low-order bending mode shapes extend throughout the entire height of the tower, and the phase and amplitude attenuation characteristics at the base measurement points are key indicators for evaluating the stiffness of the foundation constraint; hence, in addition to the top and transition sections, accelerometers must also be installed at the base. Moreover, this scheme draws on the principles proposed by Yao Wenfan (Yao, 2017), which state that sensor placement should cover the tower's critical mechanical load-transfer paths; through a multi-point layout combining the base with the upper-middle section, it successfully captures the vibration-response gradient of the tower from the constrained end to the free end, providing complete data support for modal analysis using the stochastic subspace identification method. The specific sensor locations include: the top sensor, installed on the upper platform of the hybrid tower (145 m above the foundation surface); the transition-section sensor, placed on the key platform of the steel–concrete transition segment (110 m above the foundation surface); and the base sensor, installed at the bottom of the concrete tower (0 m above the foundation surface).

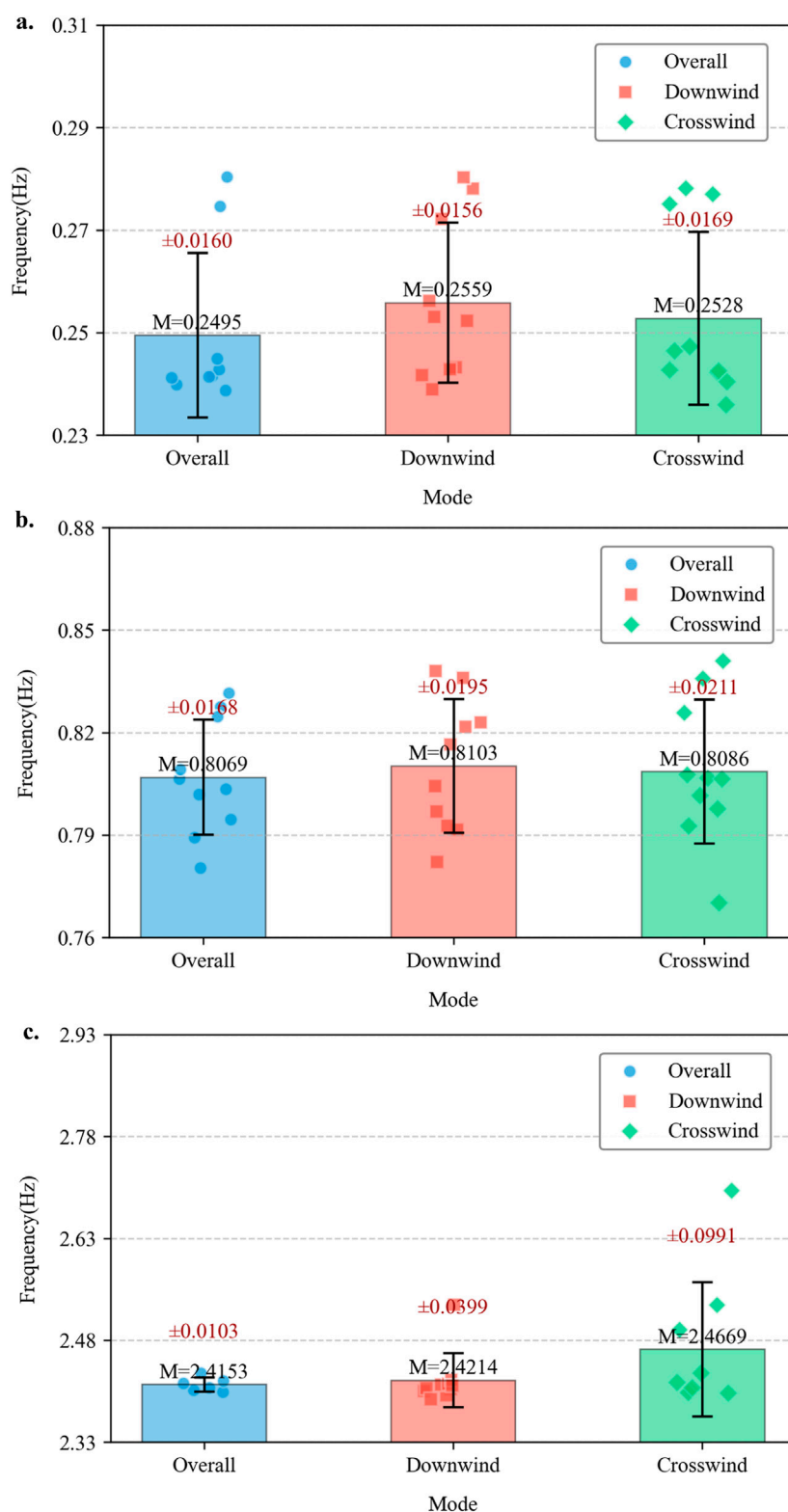
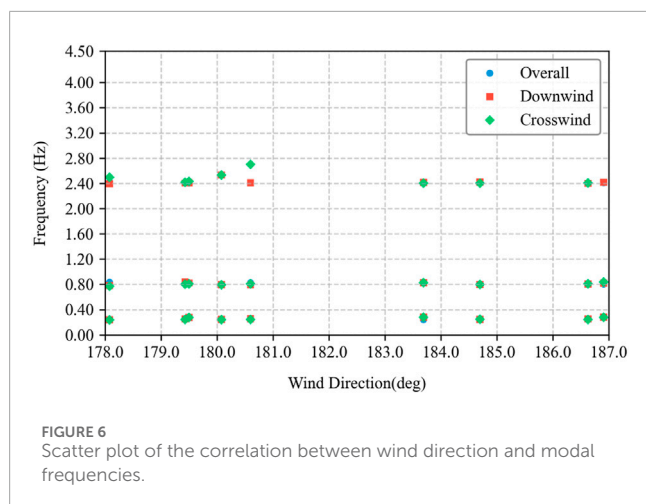


FIGURE 5 Analysis of the relationship between wind direction and frequency of wind turbine hybrid tower by SSI-COV. (a) First-order. (b) Second-order. (c) Third-order.



2.2 Operational modal analysis procedure

This study adopts a multi-stage and from-coarse-to-fine operational modal analysis procedure, as shown in Figure 2, to ensure the accuracy and reliability of the identification results.

The meteorological station of the wind farm provides daily mean wind speed, mean wind direction at 12:00, and air temperature data (see Table 3). In this study, the definition of “12:00 mean wind direction” follows the technical specifications of the turbine manufacturer: instantaneous wind-direction data collected within 15 min before or after 12:00 local standard time (11:45–12:00 or 12:00–12:15) are selected as the statistical samples, and the sampling window is determined based on data completeness (valid data ratio $\geq 95\%$). The unit-vector method is adopted for computation: each instantaneous wind direction (0° at true north, increasing clockwise) is converted into eastward and northward unit-vector components, which are averaged separately. The mean wind direction is then obtained via the arctangent function, avoiding the bias caused by the arithmetic mean when processing periodic data. After collecting the raw acceleration signals, data preprocessing is performed. A stationary vibration segment within 11:45–12:15 each day is selected, from which a 10-min high-quality segment is extracted. The X- and Y-direction data are then transformed into along-wind and cross-wind directions according to the 12:00 mean wind direction for subsequent analysis. Here, the along-wind direction corresponds to the inflow direction (FA), and the cross-wind direction to the lateral flow direction (SS).

In this study, the purpose of transforming the X- and Y-direction signals (eastward and northward) into along-/cross-wind directions according to the 12:00 mean wind direction is to focus on the vibration characteristics in the key load-bearing directions of the turbine tower. Specifically, the mean wind direction at 12:00 (converted to radians) is used together with trigonometric operations in MATLAB to rotate the original eastward and northward acceleration data into the inflow and lateral-flow coordinate system. This transformation effectively separates vibration responses dominated by wind loading from unrelated directional signals, reduces directional coupling effects on modal-identification accuracy, and ensures comparability under

varying wind directions, thereby improving the specificity and consistency of modal-parameter identification.

Preliminary modal identification adopts the Frequency Domain Decomposition (FDD) method, which is a peak-search-based technique for identifying modal parameters in the frequency domain. By detecting peaks in the power spectral density of the vibration response, the method enables preliminary identification of modal frequencies and mode shapes. It is used to determine the frequency ranges of different modal orders, evaluate data quality, and screen dates suitable for refined identification (results in Table 3). In this study, FDD is employed as a preliminary analysis step primarily to leverage its advantages of fast computation and intuitive frequency band localization, thereby providing a well-defined frequency search range for the subsequent SSI-COV analysis and significantly reducing the computational cost associated with blind parameter trials in SSI-COV.

To ensure the stability and reliability of modal identification, a “high-quality data screening” procedure is introduced at the processing stage. The screening criteria are based on the analysis of FDD spectrum features and cross-day consistency checks. The detailed steps are as follows:

1. Single-day FDD analysis: Perform frequency-domain decomposition on vibration data sampled at 200 Hz for approximately 10 min each day, obtaining FDD singular-value spectra.
2. Spectrum-feature screening: Focus on the 1–5 Hz frequency band (where low-order tower modes are concentrated) and evaluate the energy strength and clarity of singular-value peaks. If the peak energy is high, spectral lines are well-separated, and no obvious noise interference is present, the dataset is considered high quality; otherwise, data with weak, blurred, or noise-contaminated peaks are discarded.
3. Consistency verification and threshold quantification: Based on multi-day results, a threshold of singular-value peak energy $\geq 10^{-7}$ is established for determining high-quality data. The screening results are validated through cross-day consistency to ensure stable and comparable modal parameters.

Figure 3 presents a comparison between typical low-quality (August 3) and high-quality (August 4 and August 5) FDD spectra, showing that high-quality samples exhibit clear and prominent peaks in the target frequency band, verifying the rationality of the screening procedure.

For the high-quality data selected through FDD screening, 1-h acceleration data from 12:00 to 13:00 are extracted each day and analyzed using the stochastic subspace identification–covariance-driven method (SSI-COV). This method is a modal parameter identification technique defined as “a stochastic-subspace-based approach that constructs covariance matrices and performs singular-value decomposition to achieve accurate modal identification under high-noise environments.” Its “refinement” lies in the optimization of covariance-matrix construction and singular-value truncation strategies. The method provides robust estimation of modal frequencies, damping ratios, and mode shapes, and is suitable for linear systems under ambient excitation.

Before SSI-COV analysis, the data must be preprocessed through the following steps:

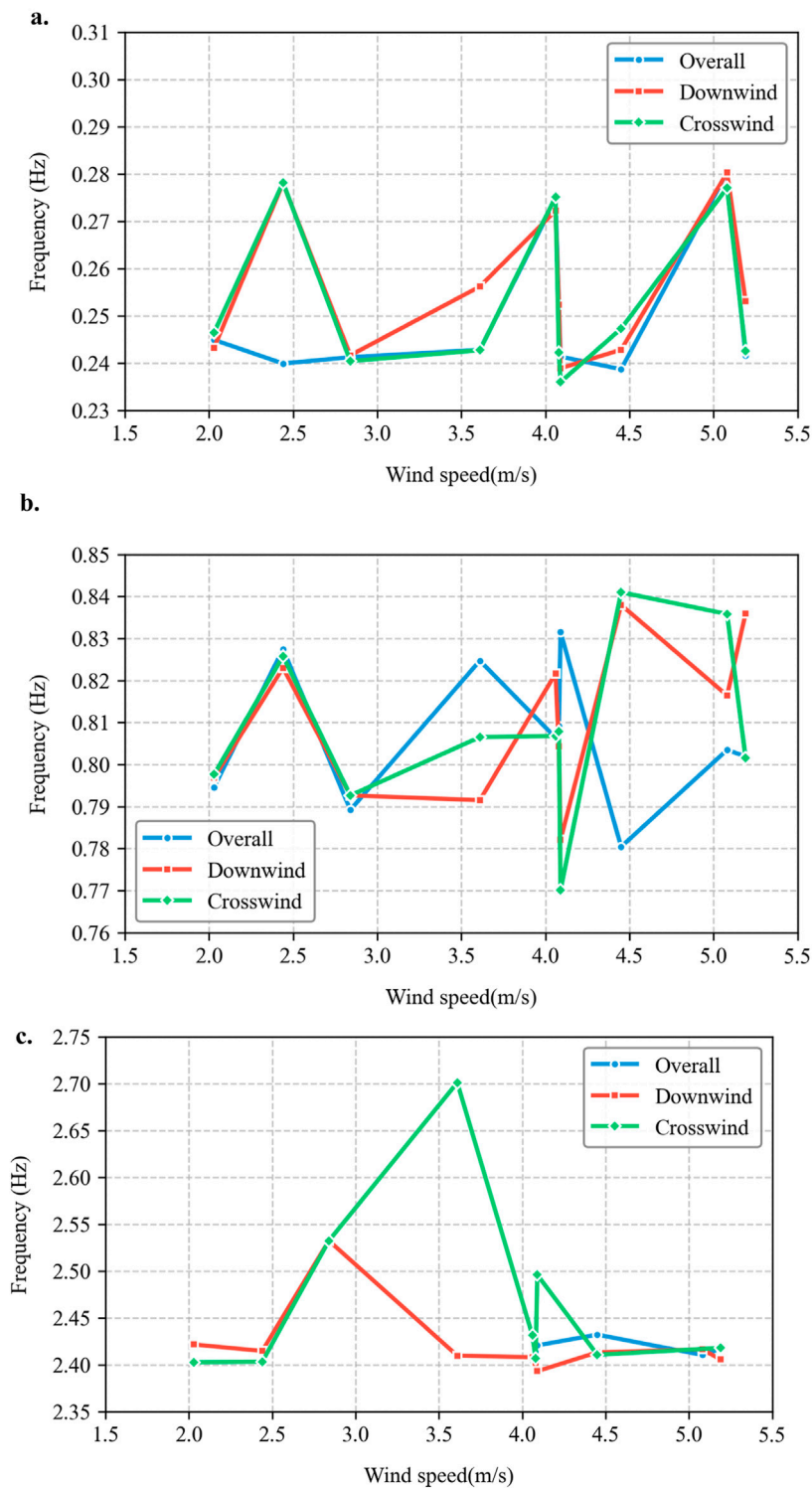


FIGURE 7 Analysis of the relationship between wind speed and frequency of wind turbine hybrid tower by SSI-COV. (a) First-order. (b) Second-order. (c) Third-order.

Detrending to remove DC offsets and slow drifts; Applying a 10 Hz low-pass filter (6th-order IIR) to retain the low-order modal band of the tower (1–5 Hz) and suppress high-frequency noise above 10 Hz, leaving a transition band for subsequent downsampling;

Anti-aliasing downsampling using the MATLAB *decimate* function (downsampling factor 20, built-in FIR anti-aliasing filter with a cutoff frequency of 4 Hz), reducing the sampling rate from 200 Hz to 10 Hz—this step further attenuates residual signals in the 5–10 Hz

TABLE 4 The temperature data recorded at 3:00 (local time) from July 28 to September 20, provided by the weather station of the wind farm.

Date	3:00 temperature/°C
20250728	28.4
20250729	28.3
20250730	28.7
20250731	26.2
20250801	26.5
20250802	27.1
20250803	28.7
20250804	31.5
20250805	31.3
20250806	32.1
20250807	29.6
20250808	29.8
20250809	27
20250810	26.1
20250811	24.9
20250812	25.4
20250813	25.9
20250814	28
20250815	29.27
20250816	31
20250817	31.7
20250818	31.5
20250819	31.3
20250820	31.6
20250821	31.27
20250822	26.3
20250823	29
20250824	28.3
20250825	27.3
20250826	26
20250827	27.9
20250828	31.4

(Continued on the following page)

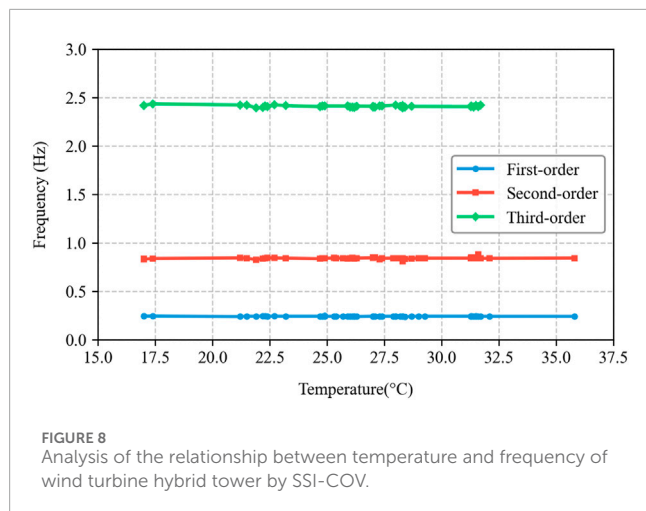
TABLE 4 (Continued) The temperature data recorded at 3:00 (local time) from July 28 to September 20, provided by the weather station of the wind farm.

Date	3:00 temperature/°C
20250829	25.3
20250830	35.8
20250831	24.8
20250901	26.2
20250902	27
20250903	28
20250904	27.4
20250905	28.2
20250906	24.7
20250907	25.7
20250908	21.9
20250909	21.5
20250910	23.2
20250911	22.7
20250912	21.2
20250913	22.4
20250914	24.9
20250915	22.3
20250916	24.9
20250917	22.2
20250918	17
20250919	17
20250920	17.4

range, strictly satisfies the Nyquist sampling criterion (Nyquist frequency 5 Hz for a 10 Hz sampling rate), avoids aliasing distortion, and reduces computational burden.

To ensure the reliability of the modal identification results, four stability criteria are employed to evaluate the consistency of each modal order across different data segments and model orders, with explicit parameter definitions as follows:

1. *Frequency deviation (eps_freq)*: the relative deviation of modal frequency under different identification conditions, within $eps_freq \in [0.001, 0.1]$, corresponding to a frequency-consistency requirement of 0.1%–10%.



2. *Damping-ratio deviation (eps_zeta)*: the absolute deviation threshold for damping ratios, set to 0.2, based on typical damping ratios of steel wind-turbine towers (0.01–0.05), allowing ~20% variation to accommodate real operating conditions.
3. *Mode-shape consistency (eps_MAC)*: measured by the Modal Assurance Criterion (MAC), within $\text{eps_MAC} \in [0.001, 0.1]$, corresponding to $\leq 10\%$ mode-shape discrepancy.
4. *Modal clustering distance (eps_cluster)*: constraining the clustering compactness of the same modal order, within $\text{eps_cluster} \in [0.1, 0.5]$, to avoid scattered or unstable solutions from affecting final modal judgment.

All parameters are validated using extensive testing on the measured tower data (1–5 Hz low-order modal range), balancing identification accuracy with real-data variability.

Furthermore, considering that harmonic excitations such as 1P and 3P during turbine operation may exhibit stability characteristics similar to structural modes in frequency, damping, and mode shape, a second-level “physical property verification” mechanism is adopted in addition to the stability criteria. Specifically:

1. *Frequency–rotational-speed correlation analysis*: suspected modal frequencies are compared with rotor rotational frequencies; if strong correlation is present, the component is classified as harmonic excitation rather than a structural mode.
2. *Mode-shape spatial-distribution verification*: true structural modes should exhibit spatial patterns consistent with tower dynamics, whereas harmonic excitations typically show uniform amplitudes across sensors or abnormal localization.

Only modes that satisfy all four stability criteria and pass the above physical-verification tests are confirmed as true structural modes; the rest are regarded as spurious modes (including 1P/3P harmonics) and are discarded.

The modal identification in this study adopts a systematic semi-automated procedure based on “parameter constraints + physical validation”. Through the aforementioned systematic identification process and strict spurious mode elimination strategy, the obtained modal parameters are ensured to have clear physical significance and engineering reliability.

2.3 Results: identified modal parameters and correlation analysis with environmental factors

2.3.1 Structural vibration parameters under wind action

Based on the results of preliminary screening by FDD and refined identification by SSI-COV, this study first systematically analyzes the modal parameter characteristics of the hybrid tower structure under wind-induced vibration.

To avoid ambiguity in direction-related terminology, this study defines the three modal frequency ranges involved in the multi-directional modal analysis as follows: the Overall modal frequency range refers to the first three modal frequencies identified from the original eastward and northward acceleration signals (without coordinate rotation); the Downwind modal frequency range corresponds to the modal frequencies along the inflow direction (FA) after coordinate transformation, aligned with the mean wind direction at 12:00 on the same day; the Crosswind modal frequency range refers to the modal frequencies along the lateral flow direction (SS), perpendicular to the 12:00 mean wind direction. These three directions share a consistent reference, reflecting the structural dynamic responses in the original coordinate system, along the primary wind-induced load direction, and along the direction perpendicular to it, respectively.

Preliminary analysis by FDD shows that the first three orders of modal frequencies of the hybrid tower exhibit interval distribution characteristics under the overall working conditions. Statistical results show that the modal frequency intervals in the overall, downwind, and crosswind directions overlap highly, and the differences are not significant, which initially indicates that wind direction changes have no systematic influence on the structural modal frequencies (Figure 4). Then, after the preliminary screening by FDD, this study conducts SSI-COV analysis on the dates selected in Table 3.

To further validate the above conclusions, this study performed refined SSI-COV identification on the high-quality data selected (Table 3). After eliminating spurious modes using stability criteria and physical validation, the first three modal frequencies were calculated under the Overall, Downwind, and Crosswind conditions. Figure 5 presents the identification results of the first three modal frequencies using a bar-scatter plot. This figure is designed to illustrate the stability of each modal order under different directions: the scatter of points reflects the identification precision, while the concentrated regions indicate the statistical distribution of modal frequencies. Each point represents an independent daily identification, with its vertical position corresponding to the frequency value. This visualization method bypasses specific time series and instead evaluates parameter stability from a statistical distribution perspective. By observing the degree of dispersion, concentration regions, and outliers, one can directly assess the quality and reliability of modal identification and obtain an intuitive basis for analyzing the influence of wind direction.

Figure 6 uses wind direction as the horizontal axis and modal frequency as the vertical axis. Each point represents an independent daily identification result and is labeled according to Overall, Downwind, and Crosswind directions. This figure quantitatively

TABLE 5 Dimensional sizes and weight of components in finite element modeling.

Component	Overall dimensions/mm	Weight/kg
Blade	Diameter 3,200, length 93,200	23,000% ± 3% per blade
Impeller (excluding blades)	4,746 × 4,233 × 4,040	51,000% ± 5%
Transmission and generator	7,545 × 3,500 × 3,250	75,000% ± 5%
Nacelle	10,900 × 4,975 × 4,050	40,000% ± 5%

TABLE 6 Center of mass position of the wind turbine rotor assembly.

Component name	Mass/t	Position (unit: m, local coordinate system)		
		x	y	z
Impeller and blades	120	5,300	0	2,314
Nacelle	40	2,523	0	2,314
Transmission and generator	75	0.8455	0	2.025

presents the variation of modal frequencies corresponding to different wind directions, providing an intuitive evaluation of the effect of wind direction changes on the first three modal frequencies.

For the first - order modal frequency, the sample sizes of the wind turbine hybrid tower under the overall, downwind, and crosswind conditions are 9, 10, and 10 respectively, and the average values of their modal frequencies are 0.2495 Hz, 0.2559 Hz, and 0.2528 Hz respectively. For the second - order modal frequency, the sample sizes of the wind turbine hybrid tower under the overall, downwind, and crosswind conditions are all 10, and the average values of their modal frequencies are 0.8069 Hz, 0.8103 Hz, and 0.8086 Hz respectively. For the third - order modal frequency, the sample sizes of the wind turbine hybrid tower under the overall, downwind, and crosswind conditions are 6, 10, and 9 respectively, and the average values of their modal frequencies are 2.4153 Hz, 2.4214 Hz, and 2.4633 Hz respectively. The maximum standard deviation among these data is ± 0.1053 , which shows that the frequency identified daily fluctuates slightly around the average value. These results all fall within the frequency interval determined by the FDD method, indicating that the identification results of the two methods are consistent and mutually verify the reliability of the analysis process. After calculation, the relative errors of each order of frequencies under the downwind, crosswind, and overall working conditions are all less than 2%, which further supports the conclusion that “wind direction has no significant impact on the modal frequency”.

Building on this, the study further analyzed the influence of wind speed variations on modal frequencies. As shown in Figure 7, within the conventional wind speed range (2.0–5.5 m/s), the modal frequencies do not exhibit a noticeable trend with increasing wind speed, indicating that wind speed has no significant effect on the structural modal frequencies.

Considering that the measured conditions in this study are mainly distributed within the low wind speed range of 2–5.5 m/s,

corresponding to the initial grid-connected generation phase between cut-in and the lower limit of rated wind speed (2.5–12 m/s), the wind turbine rotor has not yet reached a stable rated speed. The rotor speed is frequently adjusted, and both aerodynamic loading and aeroelastic effects remain weak. Under this operating state, the aerodynamic contribution to the tower stiffness is limited, making the effect of wind speed on the structure's natural frequencies difficult to observe. Therefore, no significant correlation between wind speed and the first three modal frequencies was observed within this low wind speed range.

It should be emphasized that the conclusions of this study apply only to the measured low wind speed start-up conditions and do not contradict previous literature reporting clear wind speed–modal frequency correlations in the range from rated to cut-out wind speeds. In the higher wind speed range, the turbine rotor operates at stable speed, aerodynamic loading is significantly enhanced, and aeroelastic effects clearly influence the structural dynamic characteristics, causing observable changes in modal frequencies with increasing wind speed. In contrast, under the operating conditions of this study, the aerodynamic effects are insufficient to produce changes of similar magnitude, so the correlation is not reflected in the measured data.

To improve scientific rigor and contextual clarity, this section further specifies the turbine operating states across different wind speed ranges, including: cut-in wind speed (<2.5 m/s); cut-in to rated wind speed (2.5–12 m/s, including the range of this study); rated to cut-out wind speed (12–25 m/s); cut-out wind speed (>25 m/s); and extreme wind speed (>59.5 m/s).

2.3.2 Structural vibration parameters under temperature action

On the basis of analyzing the influence of wind-induced vibration on structural dynamic characteristics, this study further explores the effect of temperature changes on the modal parameters of the wind turbine hybrid tower. Since the previous analysis has shown that wind direction and wind speed have no significant impact on structural modal frequencies, this section takes the overall structure as the research object and focuses on examining the independent influence of temperature factors.

To obtain a sufficiently wide temperature variation range and improve the reliability of the analysis, this study extended the analysis period to July 28–20 September 2025, based on meteorological data provided by the wind farm weather station (Table 4), selecting only the dates with valid monitoring records. To minimize the influence of non-temperature factors such as human activities, measurements taken at 3:00 a.m.

TABLE 7 Eccentric point mass of the wind turbine rotor assembly.

RNA Mass/t	RNA center of Mass/m	RNA rotational inertia at tower top ($I_{xx}, I_{yy}, I_{zz}, I_{zx}$)/($\times 10^6 \text{ kg}\cdot\text{m}^2$)
235	(3.41,0,2.22)	(1.16,4.84,3.68,1.83)

TABLE 8 Characteristic value of extreme loads.

F_{rk}/kN	F_{zk}/kN	M_{rk}/kN	$M_{zk}/\text{kN}\cdot\text{m}$
1,024.00	-2,305.35	8,013.50	-589.00

each day were chosen for analysis. During this period, the structure was in thermal equilibrium and external disturbances were minimal. Over the entire study period, the temperature ranged from 17.0 °C to 35.8 °C. For systematic analysis of temperature effects, the data were divided into four temperature intervals with 5 °C increments: >30 °C, 25 °C–30 °C, 20 °C–25 °C, and <20 °C.

This study conducts a statistical analysis of modal frequencies in each temperature interval. The results show that: in the >30 °C interval, the average first three-order modal frequencies are 0.242 Hz, 0.847 Hz, and 2.410 Hz respectively; in the 25 °C–30 °C interval, the corresponding values are 0.241 Hz, 0.840 Hz, and 2.408 Hz respectively; in the 20 °C–25 °C interval, they are 0.242 Hz, 0.841 Hz, and 2.412 Hz respectively; in the <20 °C interval, they are 0.243 Hz, 0.835 Hz, and 2.423 Hz respectively. It can be intuitively observed that there are no significant differences in the average first three-order modal frequencies of the wind turbine hybrid tower under different temperature intervals.

To further quantify the correlation between temperature and modal frequencies, this study plotted scatter diagrams of each modal order versus temperature and conducted linear regression analysis (Figure 8). The correlation coefficients between the first three modal frequencies and temperature variations were calculated as 0.0286, 0.0699, and 0.0978, respectively, all indicating very weak correlation. These results further confirm that, within the conventional ambient temperature range measured in this study (17 °C–36 °C), temperature variations have no significant effect on the modal frequencies of the hybrid tower wind turbine—based on the linear regression results (correlation coefficients of 0.0286, 0.0699, and 0.0978). This conclusion applies to typical atmospheric temperature ranges, and the effects under extreme temperature conditions require further investigation.

This finding holds significant engineering implications: it indicates that when conducting structural health monitoring based on vibration data, there is no need to consider the interference of ambient temperature fluctuations on frequency indicators, thereby improving the reliability and accuracy of damage identification.

3 Development of a high-fidelity finite element model

3.1 Finite element modeling strategy

In the finite element modeling of wind turbine hybrid towers, high-precision finite element models that include blades, nacelles,

and other components can account for the influence of blades on the dynamic response of the tower to a certain extent. However, the geometric shapes of nacelles, turbines, and blades are highly complex, making modeling cumbersome. Typically, the nacelle, rotor, and other components are simplified into mass points or mass blocks and applied to the top of the tower. There are multiple approaches to account for the blades. Due to the difficulty in obtaining detailed information about the blades, some researchers simplify the blade information into linear elastic cantilever beams while ignoring their mass. Additionally, since the rotation of the blades can cause singularity of the stiffness matrix, dynamic response analysis is usually only performed under the shutdown state. In practical scenarios, the geometric shape of the blades, changes in pitch angle, and rotational speed have a significant impact on the dynamic response of the wind power generation system.

In this study, the nacelle, blades, and turbine are simplified. In the actual simulation, these three components are simplified into a rectangular prism applied to the top of the tower. The mass of this rectangular prism is equal to the total mass of the three components, and the center of mass of the steel rectangular prism is consistent with that of the original structure. The total mass of all these components is 235 t. The dimensions and weights of each component are shown in Table 5.

Since information on the blades is unavailable, and variations in blade positions can also cause changes in the center of mass position, this study adopts certain simplification treatments. It is assumed that the mass of the blades is concentrated at the hub center. The total mass of the blades and hub (impeller) is 120 t, the mass of the nacelle is 40 t, and the mass of the transmission and generator inside the nacelle is 75 t. A local coordinate system is established at the top of the wind turbine, which is consistent with the yaw bearing coordinate system. The center of mass positions of each part of the wind turbine are shown in Table 6. Another local coordinate system is established at the top of the tower. After simplifying the shapes of the aforementioned components, the mass blocks are equivalent to the hub center height in accordance with the principle of consistent center of mass, and there will be a certain eccentricity in the mass blocks. The dimensions of the mass blocks are simplified based on the dimensions of the nacelle. Calculations using the center of mass formula yield: $x_c = 3.4057 \text{ m}$, $z_c = 2.2218 \text{ m}$, and $y_c = 0 \text{ m}$. Converted to the global coordinate system, the coordinates are (3.4057 m, 0 m, 159.9078 m).

The details of the blades, rotor, and nacelle are simplified into an eccentric point mass-rotational inertia simplified model (RNA), which is coupled to the top of the tower. The specific parameters of the eccentric point mass are shown in Table 7, and the reference frame for the center of mass position is the local coordinate system at the top of the tower. In the static loading analysis, the top of the hybrid tower with wet connection no longer couples the mass point. Instead, the static load application point is set at the center of the tower top surface, and the external load is applied at this loading

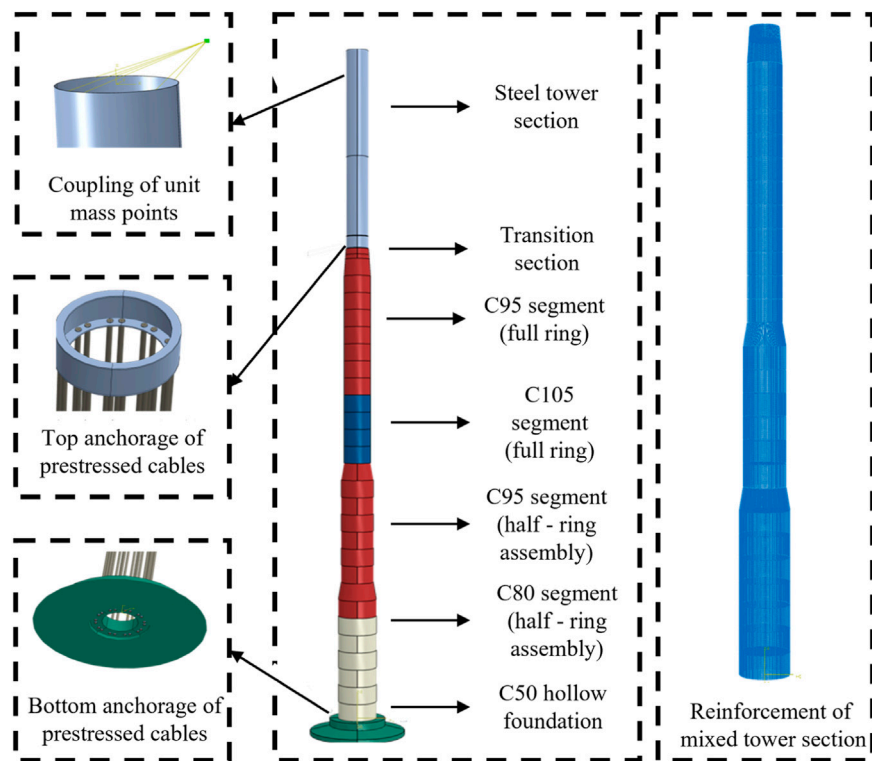


FIGURE 9
Detailed diagram of the finite element model of the wind turbine hybrid tower.

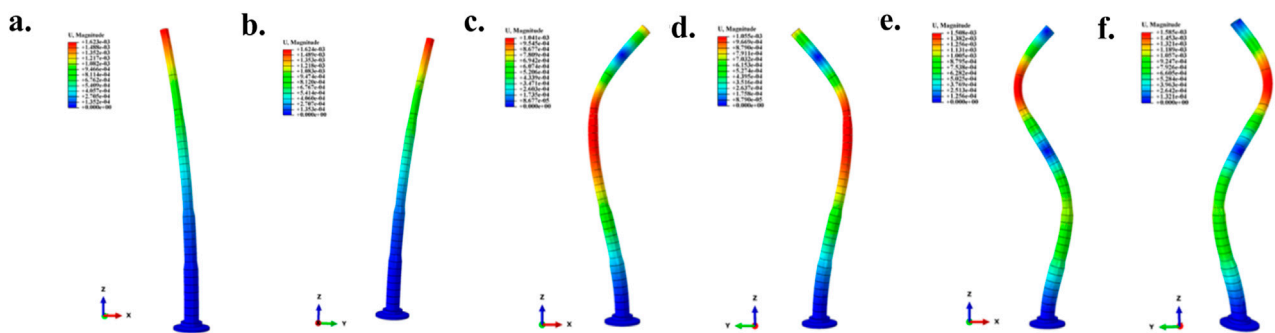


FIGURE 10
First 6 orders of natural vibration frequencies and mode shapes obtained by the Lanczos eigenvalue solver. (a) First-order lateral bending 0.235 Hz. (b) First-order fore-Aft bending 0.235 Hz. (c) Second-order lateral bending 0.939 Hz. (d) Second-order fore-Aft bending 0.939 Hz. (e) Third-order lateral bending 2.461 Hz. (f) Third-order fore-Aft bending 2.464 Hz.

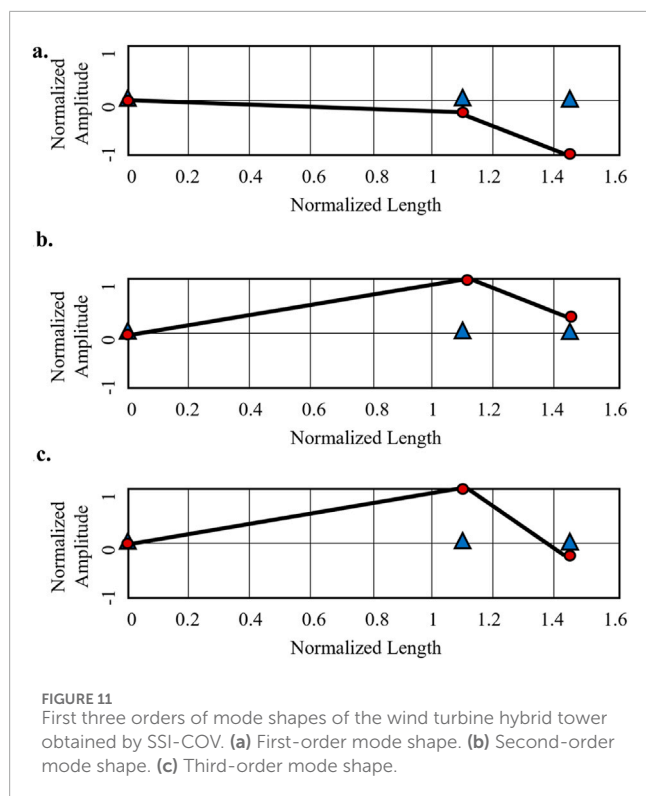
point. The loading point is coupled and bonded to the tower. The load adopts the extreme load characteristic values (excluding the safety factor) as shown in Table 8.

Based on the above engineering information, this study established an integrated finite element model of the foundation, tower, steel bars, and steel strands in ABAQUS. Details of the model are shown in Figure 9, and the simplification ideas and settings of the finite element model are summarized as follows:

1. For conservative structural design, the epoxy resin structural adhesive and positioning cones at the horizontal joints are

not considered. The contact at horizontal joints is simplified to surface-to-surface interaction with finite sliding, and the same simplification is applied between the hybrid tower and the foundation. The tangential behavior is set to penalty friction, and the normal behavior is set to hard contact. The friction coefficient between concrete-concrete interfaces is taken as 0.5, and that between concrete-steel interfaces is taken as 0.3.

2. The segments after grouting assembly have good integrity. The vertical joints are simplified to tie constraints. The steel bars at the joints are not continuous; the dowel bars are modeled



using T3D2 elements, and their interaction is simplified to Embedded region command constraints.

- The connections between the hybrid tower and the steel adapter section, between anchor bolts and the steel adapter section, and between anchor bolts and the foundation are simplified to tie constraints. The contact between the steel adapter section and S1, as well as between S1 and S2, is simplified to tie constraints.
- Steel bars are modeled using T3D2 elements, and the interaction between steel bars and concrete is simplified to Embedded region command constraints. For the elastoplastic analysis of steel bars, an ideal elastoplastic constitutive model is adopted.
- Steel strands are modeled using T3D2 elements. Their endpoints are subjected to MPC hinge constraints with the center points of the anchor bolts. Prestress is applied via the temperature reduction method, and a bilinear constitutive model is used for the elastoplastic analysis.
- The bottom surface of the foundation is assumed to have good constraint conditions, and a fixed boundary is adopted.
- Considering the influence of fluctuating wind on the tower via fluid-structure interaction is relatively complex. Instead, the wind load distributed force calculated using the formulas in the code (from Chapter 2) can be applied to the static analysis model to account for the influence of fluctuating wind on the tower wall.

3.2 Model validation: frequency and mode shape comparison

To achieve high-precision simulation of the dynamic characteristics of the wind turbine hybrid tower structure, this

study established a refined finite element model that fully considers structural details in the ABAQUS/Standard environment. The model contains a total of 409,556 elements, among which 245,736 eight-node reduced-integration solid elements (C3D8R) are used to simulate the concrete tower and foundation, and 163,820 three-node truss elements (T3D2) are employed to model the prestressed steel strand system. During the modeling process, the structural geometric dimensions, material constitutive relations, and boundary conditions were accurately reproduced. The contribution of prestress was precisely simulated by applying a tensile stress of 1,320 MPa to the steel strands.

After completing the calculation of the prestressed working condition, the Lanczos eigenvalue solver was used to extract the first 6 orders of natural frequencies and mode shapes of the tower structure, with the simulation results shown in Figure 10. The finite element analysis results indicate that the first three orders of natural frequencies of the structure are 0.235 Hz, 0.939 Hz, and 2.461 Hz, respectively.

To verify the reliability of the model, the above simulation results were compared with the operational modal analysis results based on on-site measured data in Chapter 2. The first three orders of frequencies obtained from the measurements are 0.249 Hz, 0.810 Hz, and 2.415 Hz, respectively. The relative errors of the corresponding orders are 5.62%, 15.9%, and 1.90%, respectively.

Although the error of the second-order frequency is relatively large (15.9%), which may be attributed to the complex mode shape of this order, certain uncertainties in simulating the stiffness of connection parts, or the influence of environmental noise in modal identification, the errors of the first and third-order frequencies are both controlled within 6%, and in particular, the third-order error is only 1.90%. This indicates that the model has high accuracy overall and can effectively reflect the real dynamic characteristics of the structure.

To further verify the reliability of the finite element model, this study compared the structural mode shapes obtained from on-site measured data (identified by the SSI-COV method) and numerical simulation (calculated by ABAQUS). As shown in Figure 11, the identified first three orders of experimental mode shapes and simulated mode shapes exhibit a high degree of consistency in both form and phase distribution.

The consistency of mode shapes, combined with the good matching of frequencies mentioned earlier, collectively constitutes strong evidence for verifying the accuracy of the finite element model. This result fully indicates that the established refined finite element model can not only accurately reflect the dynamic characteristics of the structure but also achieve high-precision reproduction of the actual structural behavior in terms of global mode shape features. Thus, it provides a solid theoretical foundation and numerical experimental platform for subsequent parameterized analysis, damage identification, and performance evaluation based on this model.

The experimentally validated high-accuracy finite element model not only provides a reliable platform for understanding the dynamic behavior of mixed tower structures, but also lays a solid foundation for subsequent parametric analyses, damage identification, and structural optimization, offering significant academic and engineering application value.

TABLE 9 Parameter variation of elastic modulus of concrete.

Concrete segment number	Material model	Elastic modulus/MPa	+10%/MPa	+20%/MPa	-10%/MPa	-20%/MPa
M1~M6	C80-CDP	41,707	4.59×10^4	5.00×10^4	3.75×10^4	3.34×10^4
M7~M8	UHPC120-CDP	46,208	5.08×10^4	5.54×10^4	4.16×10^4	3.70×10^4
M9~M13	C95-CDP	44,388	4.88×10^4	5.33×10^4	3.99×10^4	3.55×10^4
M14	UHPC120-CDP	46,208	5.08×10^4	5.54×10^4	4.16×10^4	3.70×10^4
M15new	C95-CDP	44,388	4.88×10^4	5.33×10^4	3.99×10^4	3.55×10^4
M16~M19	C105-CDP	46,009	5.06×10^4	5.52×10^4	4.14×10^4	3.68×10^4
M20~M28	C95-CDP	44,388	4.88×10^4	5.33×10^4	3.99×10^4	3.55×10^4

TABLE 10 Parameter variation of elastic modulus of steel.

Steel tower segment number	Material model	Elastic modulus/MPa	+10%/MPa	+20%/MPa	-10%/MPa	-20%/MPa
S1	Q355	2.1×10^5	2.31×10^5	2.52×10^5	1.89×10^5	1.68×10^5
S2	Q355	2.1×10^5	2.31×10^5	2.52×10^5	1.89×10^5	1.68×10^5

TABLE 11 Parameter variation of elastic modulus of foundation.

Foundation	Material model	Elastic modulus/MPa	+10%/MPa	+20%/MPa	-10%/MPa	-20%/MPa
Foundation	C50	3.55×10^5	3.91×10^5	4.26×10^5	3.20×10^5	2.84×10^5

4 Parametric and damage sensitivity analysis based on the validated MODEL

After obtaining an ABAQUS model that highly matches the dynamic characteristics of the actual working conditions, this study proceeds to conduct parametric analysis and damage analysis. The purpose is to explore which part of the steel-concrete hybrid tower is more sensitive to the structural dynamic characteristics, thereby providing a prerequisite for subsequent monitoring, maintenance, construction, and design.

4.1 Parametric study on key design variables

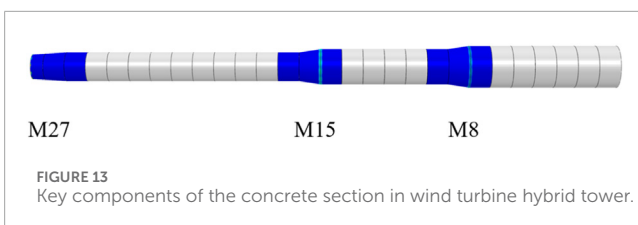
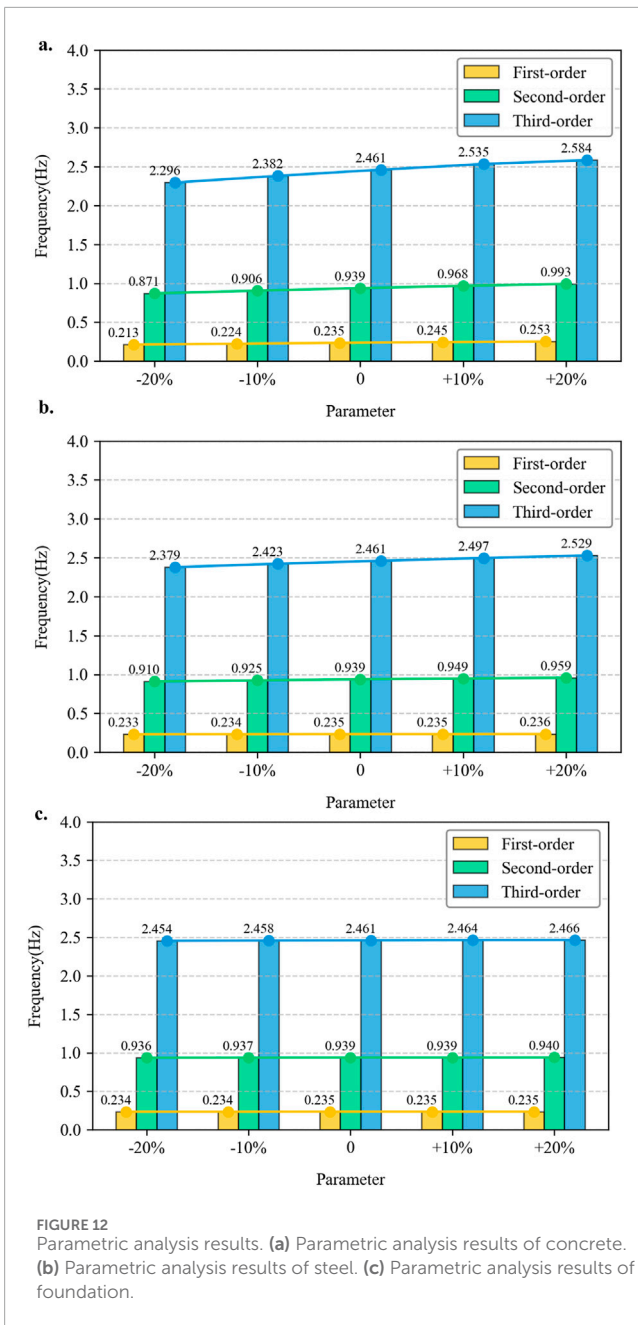
To quantify the degree of influence of key design parameters on the dynamic characteristics of the wind turbine hybrid tower, this study conducts a systematic parametric sensitivity analysis based on the validated high-precision finite element model in Chapter 3. The analysis aims to identify the parameters most sensitive to the structural natural frequencies, providing an accurate theoretical basis for structural optimization design, construction

quality control, and damage identification in future structural health monitoring.

4.1.1 Analysis parameters and working condition design

This study selects three key parameters that have a decisive impact on the overall structural stiffness for perturbation analysis: (1) Concrete elastic modulus (component names: M1–M28): Directly affects the main flexural stiffness of the hybrid tower; (2) Steel elastic modulus (component names: S1, S2): Controls the stiffness of the steel tower sections and connection parts; (3) Foundation (component name: foundation): Characterizes the interaction between the foundation and soil, and affects the system boundary conditions.

The baseline values of each parameter are determined based on actual material properties, including C80-CDP, C95-CDP, C105-CDP, and UHPC-120CDP. Among them, CDP is a constitutive model in the ABAQUS software used to simulate the damage plasticity behavior of brittle materials such as concrete; UHPC (Ultra-High Performance Concrete) refers to an advanced cement-based composite material with extremely high strength, toughness, and durability. Based on this, perturbations of -20%, -10%, +10%, and +20% are applied to each parameter respectively, as detailed



in Table 9, Table 10 and 11. The analysis strictly follows the single-variable principle—that is, when analyzing a certain parameter, the other parameters are kept at their baseline values to independently evaluate the pure influence effect of each parameter.

4.1.2 Sensitivity analysis results

The calculation results of the change rate (error) of the first three orders of structural natural frequencies relative to the baseline condition under different perturbation conditions are shown in Figure 12.

The analysis results indicate that the change in concrete elastic modulus has the most significant impact on the structural dynamic characteristics. When the concrete elastic modulus decreases by 20%, the deviations of the first three orders of modal frequencies reach as high as -9.36% , -7.24% , and -6.70% respectively. This means that the attenuation of concrete stiffness will directly lead to a significant decrease in the overall natural frequency of the structure.

In contrast, the impacts caused by changes in steel elastic modulus and foundation stiffness are relatively limited. Under the same perturbation amplitude (-20%): the deviations of the first three orders of frequencies caused by the change in steel elastic modulus are -0.851% , -3.09% , and -3.33% respectively; the deviations of the first three orders of frequencies caused by the change in foundation stiffness are even smaller, only -0.426% , -0.320% , and -0.284% respectively.

Similarly, when the concrete elastic modulus increases by 20%, the deviations of the first three orders of modal frequencies reach as high as 7.66% , 5.75% , and 5.00% respectively. Under the same perturbation amplitude ($+20\%$): the deviations of the first three orders of frequencies caused by the change in steel elastic modulus are 0.426% , 2.13% , and 2.76% respectively; the deviations of the first three orders of frequencies caused by the change in foundation stiffness are even smaller, only 0 , 0.107% , and 0.203% respectively.

4.1.3 Discussion and engineering implications

The above results clearly indicate that, in the hybrid tower structure in question, the concrete elastic modulus is the most sensitive parameter affecting its dynamic response. This phenomenon is mainly due to the fact that the concrete segments constitute the main mass and the main body of flexural stiffness of the structure; even minor changes in their mechanical properties will be significantly amplified in the overall dynamic behavior of the system.

In summary, this parametric analysis not only verifies the accuracy and reliability of the finite element model in simulating parameter changes but also provides a direct and quantitative theoretical basis for the performance evaluation and intelligent operation and maintenance of the hybrid tower structure.

4.2 Sensitivity analysis by stiffness reduction

4.2.1 Damage analysis and working condition design

Based on the aforementioned parametric analysis results, the concrete elastic modulus has been confirmed as the most sensitive parameter affecting the structural dynamic response. To further explore the impact of concrete component damage on the overall dynamic characteristics, this study conducts a targeted damage sensitivity analysis. Finite element analysis results show that under operational loads, the steel bar stress concentration in the concrete tower mainly occurs at the variable-diameter segment joint areas

with sudden geometric changes, including the M8, M15, and M27 sections. Among these, the maximum Mises stress value is 329.5 MPa, which appears on the lower compression side of the steel mesh in the M15 variable-diameter segment.

This stress concentration phenomenon reveals the potential risks of the aforementioned sections under complex loads. To quantify the impact of these local areas on the overall dynamic performance of the structure, this study selects three key components—M8, M15, and M27—as representative regions (Figure 13). Different degrees of damage states are simulated by introducing 10%, 20%, 30%, 40%, and 50% elastic modulus reduction (i.e., stiffness degradation) into their material constitutive models. By calculating the changes in structural natural frequencies under each damage condition relative to the intact baseline model, the sensitivity of the impact of damage location and degree on the global dynamic characteristics is systematically evaluated.

4.2.2 Damage analysis results

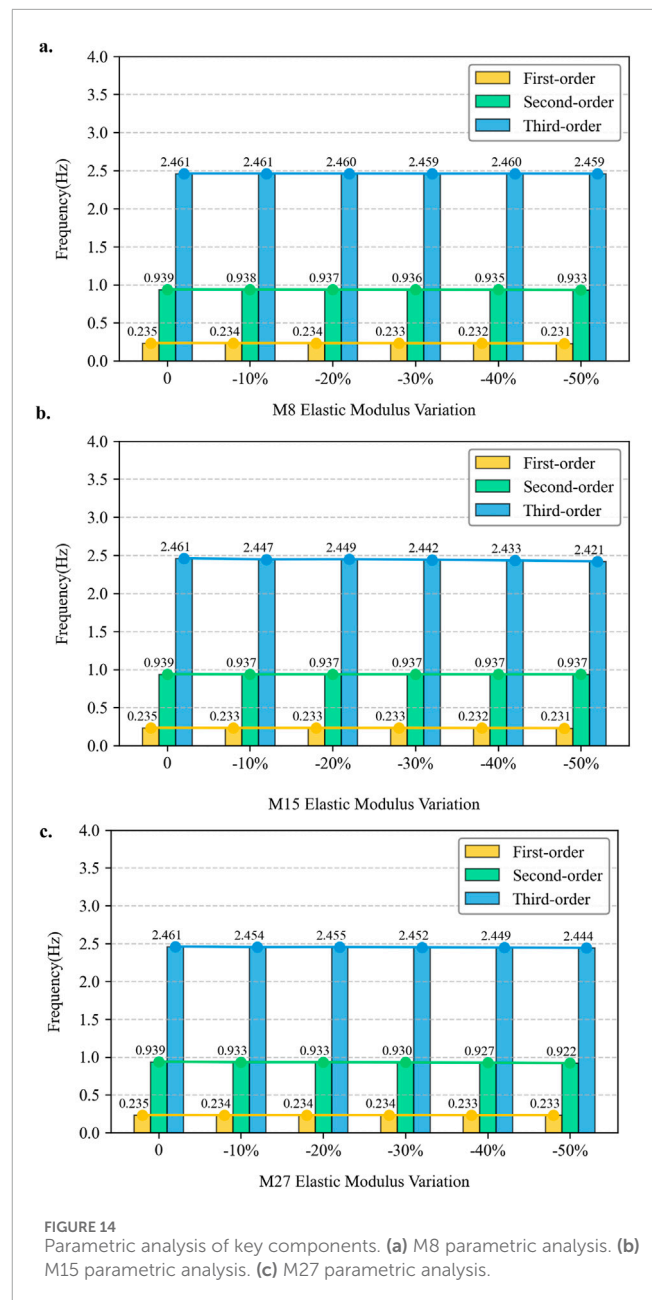
Under different working conditions, the damage status of the steel-concrete hybrid tower is shown in Figure 14 (absolute values of errors are used for intuitive presentation), and the following conclusions can be drawn:

1. Impact of damage location specificity: The impact of damage on frequencies of different orders shows significant location specificity. Damage in the M15 section has the most significant impact on the third-order frequency: when the stiffness of the M15 section is reduced by 50%, the third-order frequency deviation reaches as high as 1.625%, which is much greater than its impact on the first and second-order frequencies. This indicates that the third-order mode shape has large deformation in the M15 area, and damage in this section can be most effectively captured by the change in the third-order frequency. Damage in the M27 section has a prominent impact on the second-order frequency: damage in the M27 section is also more sensitive to higher-order frequencies; when the stiffness is reduced by 50%, the second-order frequency deviation is 1.810% and the third-order frequency deviation is 0.691%, highlighting its strong correlation with the second-order mode shape.
2. Low-order frequencies are insensitive to damage: The analysis shows that the change in the first-order frequency is very small under all damage conditions (the maximum deviation is only 0.170%). This indicates that relying solely on the fundamental frequency for damage identification may not be sensitive enough, and it is easy to miss local damage. Therefore, it is necessary to combine high-order frequency information for comprehensive judgment.

4.2.3 Discussion and engineering implications

The core finding of the damage analysis in this study is that the impact of damage on structural dynamic characteristics exhibits an obvious “location-order” correspondence. This finding provides a crucial theoretical basis for structural health monitoring based on vibration data:

Damage localization: By monitoring the variation patterns of frequencies across multiple orders, a correlation can be established



with specific damage locations. For example, if the monitoring system detects a significant decrease in the third-order frequency while the first and second-order frequencies show minimal changes, it can provide an initial early warning that damage may be located near the M15 section.

Sensor placement optimization: The analysis results indicate that low-order frequencies are insensitive to local damage. Therefore, in health monitoring systems, it is necessary to adopt advanced algorithms capable of accurately identifying high-order modes and high-sensitivity sensors to enhance the ability to detect early-stage local damage.

In summary, this damage sensitivity analysis not only verifies the effectiveness of the finite element model in simulating damaged working conditions but, more importantly, reveals the great potential of using changes in dynamic characteristics for damage

identification and localization. It lays a solid theoretical foundation for the subsequent development of a targeted health monitoring system for hybrid tower structures.

5 Conclusion and limitations

5.1 Conclusion

This study conducts a systematic and comprehensive research on the dynamic characteristics of a certain wind turbine hybrid tower through on-site measurements, operational modal analysis, high-precision finite element simulation, and parametric research. The main research work and conclusions are as follows:

1. The influence mechanism of environmental factors on modal parameters is verified. Through a rigorous on-site measurement and data analysis process (including FDD and SSI-COV methods), this study empirically confirms that within the range of conventional environmental changes (wind speed: 2.0m/s-5.5 m/s; 17°C–35.8 °C), environmental factors (wind direction, wind speed, temperature) have no significant impact on the modal frequencies of the hybrid tower structure. This conclusion provides a crucial prerequisite for structural health monitoring (SHM) based on vibration monitoring—specifically, significant changes in modal frequencies can be attributed to damage such as structural stiffness degradation, rather than interference caused by conventional environmental changes, thereby greatly improving the reliability of damage identification. It should be noted that the conclusion of this study—that “the concrete elastic modulus has the most significant impact on the inherent vibration characteristics of the tower”—applies only to the 160 m steel-concrete hybrid tower analyzed here. Its applicability to towers of other heights or structural types requires further verification.
2. An experimentally validated finite element model was established. Based on the ABAQUS platform, this study constructed a FE model of the wind turbine hybrid tower. Verified by on-site measured data, the model exhibits excellent capability in predicting dynamic responses. On this basis, the study further utilized this validated model to systematically conduct parametric and damage sensitivity analyses.
3. The dominant influence of concrete material parameters on the structural dynamic characteristics was revealed. Through systematic parametric analysis of key parameters such as concrete properties, steel properties, and foundation stiffness, it was found that variations in the elastic modulus of concrete have the most significant impact on the overall natural vibration characteristics of the structure. Its sensitivity is far higher than that of changes in the elastic modulus of steel and foundation stiffness. This conclusion clearly indicates that in the structural health monitoring of hybrid towers, the performance degradation of concrete structures should be taken as the core focus, providing a key basis for the formulation of monitoring strategies.
4. A clear corresponding relationship between damage location and frequency order was identified. Based on the stress

analysis results, damage sensitivity analysis conducted on key sections such as M8, M15, and M27 showed that the influence of stiffness degradation at different locations on the natural frequencies of each order presents a significant “location-order” correlation (e.g., damage in the M15 section has the most prominent impact on the third-order frequency). This finding theoretically confirms the feasibility of using multi-order frequency variation patterns to achieve damage localization and quantitative assessment, laying a solid theoretical foundation for the development of damage identification methods for hybrid tower structures based on vibration data.

5.2 Limitations and future work

The on-site measurement data cycle of this study can be further extended to cover more extreme seasonal climate conditions. Future research can develop a structural health monitoring system dedicated to wind turbine hybrid towers based on this high-precision model and the results of damage sensitivity analysis, realizing online damage identification and safety early warning. Additionally, the research method can be extended to other types of hybrid structure systems.

Data availability statement

The original contributions presented in the study are included in the article/supplementary material, further inquiries can be directed to the corresponding author.

Author contributions

KX: Data curation, Funding acquisition, Writing – review and editing. ZZ: Resources, Writing – review and editing. ST: Investigation, Methodology, Software, Validation, Writing – original draft. WJ: Investigation, Writing – original draft. GL: Project administration, Writing – review and editing. JX: Conceptualization, Funding acquisition, Project administration, Supervision, Writing – review and editing.

Funding

The author(s) declared that financial support was received for this work and/or its publication. This research was funded by the Project of Research on Safety Intelligent Monitoring and Evaluation of Ultra-high Wind Turbine Steel/Hybrid Tower Tubes (2025GKF-0536) and 111 Project (B20039).

Conflict of interest

Authors KX and ZZ were employed by Shandong Electric Power Engineering Consulting Institute Corp., Ltd.

Author WJ was employed by Tianjin Qiushi Intelligent Technology Corp., Ltd.

The remaining author(s) declared that this work was conducted in the absence of any commercial or financial relationships that could be construed as a potential conflict of interest.

The author JX declared that they were an editorial board member of Frontiers, at the time of submission. This had no impact on the peer review process and the final decision.

Generative AI statement

The author(s) declared that generative AI was not used in the create of this manuscript.

References

- Aikhuele, O., and Diemuodeke, O. E. (2024). Computational analysis of stiffness reduction effects on the dynamic behaviour of floating offshore wind turbine blades. *J. Mar. Sci. Eng.* 12 (10), 1846. doi:10.3390/jmse12101846
- Asmine, M., Brochu, J., Fortmann, J., Gagnon, R., Kazachkov, Y., Langlois, C.-E., et al. (2010). Model validation for wind turbine generator models. *IEEE Trans. Power Syst.* 26 (3), 1769–1782. doi:10.1109/TPWRS.2010.2052867
- Bórawski, P., Beldycka-Bórawska, A., Jankowski, K. J., Dubis, B., and Dunn, J. W. (2020). Development of wind energy market in the european union. *Renew. Energy* 161, 691–700. doi:10.1016/j.renene.2020.07.081
- Brincker, R., and Ventura, C. (2015). *Introduction to operational modal analysis*. John Wiley and Sons.
- Burton, T., Jenkins, N., Sharpe, D., and Bossanyi, E. (2011). *Wind energy handbook*. John Wiley and Sons.
- Cheng, Y., Zhao, Y., Qi, H., and Zhou, X. (2024). Intelligent optimal design of steel-concrete hybrid wind turbine tower based on evolutionary algorithm. *J. Constr. Steel Res.* 218, 108729. doi:10.1016/j.jcsr.2024.108729
- Ciang, C. C., Lee, J.-R., and Bang, H.-J. (2008). Structural health monitoring for a wind turbine system: a review of damage detection methods. *Meas. Sci. Technol.* 19 (12), 122001. doi:10.1088/0957-0233/19/12/122001
- Dong, X. F., Lian, J. J., Yang, M., and Wang, H. J. (2014). Operational modal identification of offshore wind turbine structure based on modified stochastic subspace identification method considering harmonic interference. *J. Renew. Sustain. Energy* 6 (3). doi:10.1063/1.4875462
- Farrar, C. R., and Worden, K. (2012). *Structural health monitoring: a machine learning perspective*. John Wiley and Sons.
- Global Wind Energy Council (2021). *GWEC global wind report 2021*. Brussels, Belgium: Global Wind Energy Council, 80.
- Jia, K. Q., Zhang, Z. L., Liu, Z. T., Gao, X. F., and Xu, J. (2025). Mechanical performance analysis of wet - connected prefabricated steel - concrete composite tower. *Wind Energy* 2025 (01), 76–84. doi:10.3969/j.issn.1674-9219.2025.01.017
- Lantz, E., Roberts, O., Nunemaker, J., DeMeo, E., Dykes, K., and Scott, G. (2019). *Increasing wind turbine tower heights: opportunities and challenges*. Golden, CO, USA: National Renewable Energy Laboratory.
- Lenzen, A., Rohrer, M., and Vollmering, M. (2021). Damage localization of mechanical structures considering environmental and operational conditions based on output-only system identification and H-estimation. *Mech. Syst. Signal Process.* 156, 107572. doi:10.1016/j.ymssp.2021.107572
- Liu, Q. Y., Jia, K. Q., Chu, H. M., Jiang, W. T., Ye, C. J., and Xu, J. (2023). "Finite element analysis and structural optimization of hybrid tower wind turbine foundation," in *Proceedings of the 23rd national symposium on modern structural engineering*, 234–239.
- Liu, Q. Y., Li, S. B., Jia, K. Q., Jiang, W. T., Liu, Z. T., and Xu, J. (2024). Application of prestressing technology in the foundation slab of circular wind turbine units. *Wind Energy* 2024 (01), 66–72. doi:10.3969/j.issn.1674-9219.2024.01.016
- Mosavi, A. A., Seracino, R., and Rizkalla, S. (2012). Effect of temperature on daily modal variability of a steel-concrete composite bridge. *J. Bridge Eng.* 17 (6), 979–983. doi:10.1061/(ASCE)BE.1943-5592.0000416
- Any alternative text (alt text) provided alongside figures in this article has been generated by Frontiers with the support of artificial intelligence and reasonable efforts have been made to ensure accuracy, including review by the authors wherever possible. If you identify any issues, please contact us.
- Publisher's note**
- All claims expressed in this article are solely those of the authors and do not necessarily represent those of their affiliated organizations, or those of the publisher, the editors and the reviewers. Any product that may be evaluated in this article, or claim that may be made by its manufacturer, is not guaranteed or endorsed by the publisher.
- Partovi-Mehr, N., Branlard, E., Bajric, A., Liberatore, S., Hines, E. M., and Moaveni, B. (2022). *Sensitivity of modal parameters of an offshore wind turbine to operational and environmental factors: a numerical study*. Golden, CO, USA: National Renewable Energy Lab NREL.
- Pei, X. Y., Huang, H. B., and Cao, P. (2025). An improved Gaussian mixture model-based data normalization method for removing environmental effects on damage detection of structures. *Buildings* 15 (3), 359. doi:10.3390/buildings15030359
- Rainieri, C., and Fabbrocino, G. (2014). *Operational modal analysis of civil engineering structures*. New York: Springer.
- Reuland, Y., Martakis, P., and Chatzi, E. (2023). A comparative study of damage-sensitive features for rapid data-driven seismic structural health monitoring. *Appl. Sci.* 13 (4), 2708. doi:10.3390/app13042708
- Reynders, E. (2012). System identification methods for (operational) modal analysis: review and comparison. *Archives Comput. Methods Eng.* 19 (1), 51–124. doi:10.1007/s11831-012-9069-x
- Ribeiro, J. A., Ribeiro, B. A., Pimenta, F., Tavares, S. M. O., Zhang, J., and Ahmed, F. (2025). Offshore wind turbine tower design and optimization: a review and AI-driven future directions. *Appl. Energy* 397, 126294. doi:10.1016/j.apenergy.2025.126294
- Sharma, V. B., Singh, K., Gupta, R., Joshi, A., Dubey, R., Gupta, V., et al. (2021). Review of structural health monitoring techniques in pipeline and wind turbine industries. *Appl. Syst. Innov.* 4 (3), 59. doi:10.3390/asi4030059
- Sohn, H. (2007). Effects of environmental and operational variability on structural health monitoring. *Philosophical Trans. R. Soc. A Math. Phys. Eng. Sci.* 365 (1851), 539–560. doi:10.1098/rsta.2006.1920
- Tapoglou, E., Georgakaki, A., Prior, A. R., and Govern, L. M. C. (2025). Knowledge gaps in the wind energy technology supply chain.
- Van de Graaf, T. (2014). "The international energy agency," in *Handbook of governance and security* (Cheltenham, United Kingdom: Edward Elgar), 489–503.
- Wiser, R., Bolinger, M., Hoen, B., Millstein, D., Rand, J., Barbore, G., et al. (2023). *Land-based wind market report*. 2023 edition.
- Yang, Y., Liang, F., Zhu, Q., and Zhang, H. (2024). An overview on structural health monitoring and fault diagnosis of offshore wind turbine support structures. *J. Mar. Sci. Eng.* 12 (3), 377. doi:10.3390/jmse12030377
- Yao, W. (2017). *Wind turbine structural vibration monitoring and early warning methods*. Harbin, China: Harbin Institute of Technology. Master's thesis.
- Zhang, M., Chen, H., Yan, T., Sun, H., and Wu, L. (2023). Research on improved modal parameter identification method using hilbert-huang Transform. *Meas. Control* 56 (9–10), 1637–1648. doi:10.1177/00202940231173752
- Zhang, Z., Liu, Q., Chu, H., Lacidogna, G., Xu, J., Cheng, H., et al. (2023). Performance analysis of an improved gravity anchor bolt expanded foundation. *Appl. Sciences* 13 (20), 11181. doi:10.3390/app13201181
- Zhang, M., Liu, B., Gao, C., Hossain, Md N., and Zhao, G. (2024). Wind-induced response analysis and fatigue reliability study of a steel-concrete composite wind turbine tower. *Buildings* 14 (6), 1740. doi:10.3390/buildings14061740